PHYSICAL REVIEW B VOLUME 39, NUMBER 8 15 MARCH 1989-I

Magnetocapacitance measurements of subband separation in an accumulation layer on n^--type GaAs

T. W. Hickmott
IBM Research Division, Thomas J. Watson Research Center, P.O. Box 218, Yorktown Heights, New York 10598
(Received 13 September 1988)

Magnetocapacitance measurements on an n^--type GaAs undoped $Al_xGa_{1-x}As/n^+$-type GaAs (AlGaAs) capacitor are used to determine the subband separation E_1-E_0 for an accumulation layer on n^--type GaAs. For values of surface electron concentration N_S large enough that two subbands can be occupied, and for certain values of magnetic field, B, Landau levels in the lowest subband coincide with those in the first excited subband. The result is a characteristic sequence of maxima in the density of states at the Fermi level which is detected as a sequence of maxima in magnetocapacitance curves of an AlGaAs capacitor. For the sample studied, E_1-E_0 varies between 24.5 and 33.5 meV for $8.9\times10^{11}<N_S<13.1\times10^{11}$ cm^2, somewhat less than calculated values.

INTRODUCTION

When an accumulation layer or an inversion layer forms at a semiconductor-insulator interface, carrier motion perpendicular to the interface is confined while carriers can move freely parallel to the interface.[1] A sequence of electric subbands forms whose energy separation and occupation depend on the carrier concentration N_S in the two-dimensional electron gas (2D EG) at the interface. At low temperatures and low values of N_S only the lowest subband, E_0, is populated. As N_S increases the Fermi level of the 2D EG increases and higher subbands, $E_1, E_2, \ldots$ are occupied. The occupation of higher subbands affects many properties of the 2D EG, though often in subtle ways.[2-9] The determination of the onset of occupation of a second subband and its energy separation, $E_{10}=E_1-E_0$, is an important problem in characterizing two-dimensional electron gases on semiconductors. In the present paper E_1-E_0 in an accumulation layer on n^--type GaAs is determined as a function of N_S from structure observed in magnetocapacitance curves of an n^--type GaAs/undoped $Al_xGa_{1-x}As/n^+$-type GaAs (AlGaAs) capacitor. The energy separation of subbands is obtained in terms of the Landau level separation in the accumulation layer. This is the first use of magnetocapacitance measurements in a heterostructure to determine the dependence of subband separation on N_S.

There are several theoretical calculations of subband energies of $GaAs/Al_xGa_{1-x}As$ heterostructures.[10-12] Experimental determinations of subband energies have been primarily optical, either by Raman scattering[13,14] or by cyclotron resonance at infrared energies.[15-20] Most determinations have been on modulation-doped $GaAs/Al_xGa_{1-x}As$ structures which have a limited range of N_S, although recently front-gated modulation-doped heterostructures have been studied in which N_S can be varied between 1×10^{10} and 5×10^{11} cm^{-2}.[18-20] Smith *et al.*[9] have determined E_1-E_0 at the onset of occupation of a second subband from magnetotransport measurements of conductance of a 2D EG at a $GaAs/Al_xGa_{1-x}As$ interface.

One of the simplest structures for studying the properties of a 2D EG on GaAs is the AlGaAs capacitor, shown schematically in Fig. 1(a), in which an undoped $Al_xGa_{1-x}As$ layer serves as a dielectric between n^--type GaAs and n^+-type GaAs layers.[21,22] An accumulation layer forms on n^--type GaAs when a positive gate bias V_G is applied to the n^+-type GaAs gate of the AlGaAs capacitor. The AlGaAs capacitor is nearly ideal. The interface state density at the n^--type GaAs/$Al_xGa_{1-x}As$ interface is $\lesssim10^{10}$ cm^{-2}; for temperatures greater than 100 K the capacitance-voltage (C-V) characteristics can be accurately modeled by classical semiconductor-insulator-semiconductor theory.[21] The surface electron concentration can be varied from depletion through zero at the flat-band voltage V_{FB} to values greater than 1×10^{12} cm^{-2} by increasing V_G. The maximum value of N_S is determined by the maximum value of V_G which is limited by tunneling through the $Al_xGa_{1-x}As$ layer.

Two subbands, E_0 and E_1, are indicated in the accumulation layer in Fig. 1(a). As shown schematically by the dotted lines in Fig. 1(b) the density of states (DOS) of each subband in a 2D EG is constant in energy if $B=0$.[1] For each subband $D(E)=g_v m^*/\pi\hbar^2$ (cm^{-2} eV^{-1}) where g_v is the valley degeneracy (1 for GaAs), m^* is the electron effective mass, and $\hbar$ is Planck's constant. As V_G increases, N_S in the 2D EG of the accumulation layer increases and the Fermi energy E_F, measured from the bottom of the lowest subband, increases. When $E_F>E_{10}$, electrons begin to populate the first excited subband, E_1. The total density of states at E_F when $E_F>E_1$ is twice that when $E_F<E_1$. When a magnetic field B is applied perpendicular to the accumulation layer the constant density of states is replaced by a sequence of Landau levels whose energies are

$$E_{i,N}=E_i+(N+\tfrac{1}{2})\hbar\omega_c\pm\tfrac{1}{2}g\mu_B B,\quad i,N=0,1,2,\ldots, \qquad (1)$$

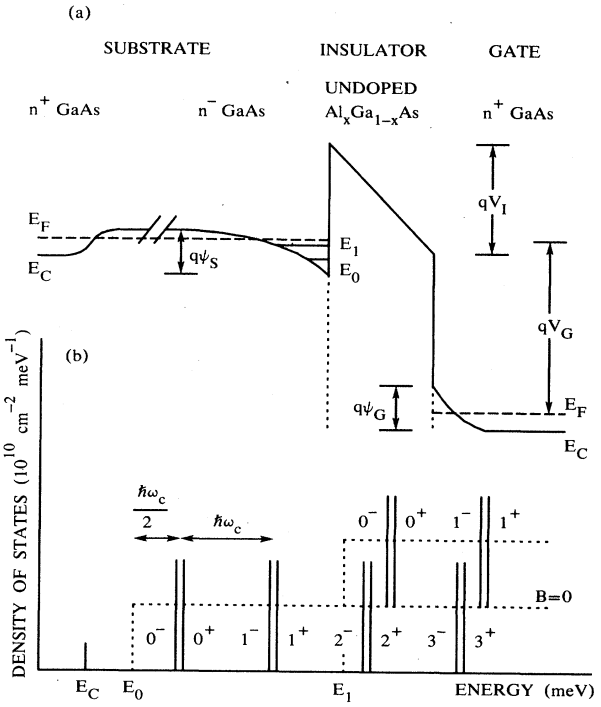

FIG. 1. (a) Schematic energy band diagram for n^--type GaAs/$Al_xGa_{1-x}As$/n^+-type GaAs capacitor in accumulation, showing two subbands. (b) Schematic energy dependence of density of states in a two-dimensional electron gas when $B=0$ T (dotted lines) or when $B>0$ T (vertical lines).

where E_i is $E_0, E_1, \ldots$, the energy of the bottom of each subband when $B=0$ T, N is the Landau level index, μ_B is the free electron Bohr magneton, and g is the g factor of the electrons in the accumulation layer. The Landau level separation is $\hbar\omega_c = e\hbar B/m^*$ where e is the electron charge. The notation E_{i,N^+} or E_{i,N^-} will be used to designate particular spin-split Landau levels, for example, $E_{0,2^+}$ or $E_{1,0^-}$. Landau levels are shown schematically as δ functions in Fig. 1(b); spin levels for each N are indicated by $+$ and $-$. The number of carriers per Landau level, with spin splittings resolved, is

$$N_L = \frac{eB}{h} = 2.418\times10^{10}B\,[\mathrm{T}]\ \mathrm{cm}^{-2}\ . \tag{2}$$

The model of Fig. 1(b) is highly idealized and is correct only at $T=0$ K. At finite temperatures and in real systems Landau levels are broadened by inhomogeneities or scattering. The determination of the energy dependence of the DOS of a 2D EG in a magnetic field has been a major problem in the GaAs/$Al_xGa_{1-x}As$ system. Magnetization, specific heat, activated transport, and magnetocapacitance measurements show that there is a significant DOS between Landau levels, at least in modulation-doped heterostructures.[23] There have been no similar studies of the DOS of a 2D EG in an accumulation layer on GaAs.

The AlGaAs capacitor of Fig. 1(a) is well suited for magnetocapacitance measurements. The total capacitance C_T is given by

$$\frac{1}{C_T} = \frac{1}{C_I} + \frac{1}{C_G} + \frac{1}{C_S}\ , \tag{3}$$

where C_I is the capacitance of the insulating $Al_xGa_{1-x}As$ layer, C_G is the capacitance of the n^+-type GaAs gate, and C_S is the capacitance of the n^--type GaAs substrate. All capacitances are per unit area. It is necessary to include C_G since band bending in the gate ψ_G is comparable to ψ_S, the band bending in the substrate, for AlGaAs capacitors when an accumulation layer forms on n^--type GaAs.[24] Following the initial work of Voshchenkov and Zemel[25] on magnetocapacitance of Si metal-oxide-semiconductor field-effect transistors (MOSFET's), Stern[26] showed that $1/C_S$ is related to the density of states at the Fermi level,[27–30]

$$\frac{1}{C_S} = \frac{\gamma z_0}{\epsilon_S} + \frac{1}{e^2[dN_S/d(E_F-E_0)]_{E_F}}\ , \tag{4}$$

where γ is a constant between 0.5 and 0.7, z_0 is the average position of electrons in the 2D EG, ϵ_S is the dielectric constant of the semiconductor, and $[dN_S/d(E_F-E_0)]_{E_F}$ is the thermodynamic density of states at the Fermi level. From Eqs. (3) and (4), maxima (minima) in the density of density of states result in maxima (minima) in the total capacitance if C_I and C_G remain constant. Smith *et al.*[27] have used minima in magnetocapacitance curves to obtain a density of states in modulation-doped heterostructures while Mosser *et al.*[29] have used maxima for the same purpose. Smith *et al.*[28] were able to fit the whole magnetocapacitance curve below 5 T with a suitable density of states. In the present paper we show that E_1-E_0 in an accumulation layer can be obtained from maxima of curves of capacitance measured at constant V_G as B is varied (C-V-B curves).

For the AlGaAs capacitor in Fig. 1(a), N_S for an accumulation layer depends on the electric field F_S at the n^--type GaAs/$Al_xGa_{1-x}As$ interface. For fixed V_G, the voltage across the insulator, V_I, band bending in the substrate, and band bending in the gate, are nearly constant as B changes; therefore N_S is nearly constant. Because the population of each spin-split Landau level is proportional to B, if N_S is constant the Fermi level makes abrupt jumps as one Landau level becomes filled and a different level is occupied.[31,32] Figure 2 shows a sequence of Landau level diagrams for $N_S=1.1\times10^{12}$ cm^{-2}, $E_1-E_0=30$ meV, and $g=3.0$. In Fig. 2 the zero of energy corresponds to E_0 at 0 T. The height of each Landau level is proportional to its degeneracy at each value of B. Its energy is determined from Eq. (1) using $m^*=0.067$. The dotted line shows the Landau level in which the Fermi level is located. At 12.0 T, E_F is in the 1^+ spin level of the lowest subband which is designated as $E_{0,1^+}$; as B is reduced to 10.0 T E_F has shifted to the $E_{1,0^-}$ spin level of the first excited subband. At 9.2 T, shown in Fig. 2(c), E_F remains in the $E_{1,0^-}$ level but Landau levels of the lowest subband, with $N=2$, approach the energy of the $E_{1,0^-}$ level. At 8.8 T, E_F shifts into the $E_{0,2^-}$ level, at 8.6 T it shifts back into the $E_{1,0^-}$ level. At

some B between 8.6 and 8.8 T, the $E_{0,2^-}$ and $E_{1,0^-}$ levels coincide and there is a doubling of the density of states at the Fermi level. As B is further reduced, E_F shifts into the $E_{0,2^+}$ level, then into the $E_{1,0^-}$ level of the upper subband, and the sequence repeats itself with the $N=3$ Landau levels of the lowest subband as B is reduced further.

The abrupt jumps in E_F corresponding to its shifting from one Landau level to another as B changes are shown by the solid line in Fig. 3(a) which is a plot of E_F-E_0 versus B for the same values of N_S, E_1-E_0, and g as in Fig. 2. The dotted lines show the energies of different spin-split Landau levels of E_0 and E_1. E_F follows these lines for ranges of B until complete filling or emptying of a level requires a jump of E_F to the next Landau level. The pattern of changes of Fermi level is complex, particularly when spin splitting is included. For the sample used in this work there is good electrical contact to a voltage source through the n^+-type GaAs wafer. In such a case the Fermi level stays fixed but the subbands move to accommodate changes in E_F-E_0. The reality of the jumps of E_F is demonstrated by recent measurements of the potential variations in a floating-gate GaAs structure with changing magnetic field.[33,34]

The δ-function Landau levels of Fig. 2 are highly idealized. Gaussian broadening of Landau levels has been generally used in deriving a DOS from experimental data.[23,28,29] To convert from an energy scale in Fig. 2 to a magnetic field scale, we have used a model Gaussian density of states of the form

$$D(E)=\frac{eB}{h}\sum_{i,N}\frac{1}{\Gamma}\left[\frac{2}{\pi}\right]^{1/2}\exp\left[-\frac{2(E-E_{i,N})^2}{\Gamma^2}\right] \quad (5)$$

to calculate the density of states at the Fermi level as a function of B. Γ is the broadening parameter and $E_{i,N}$ is the energy of each spin-split Landau level. Results are shown in Fig. 3(b) for $\Gamma=0.6$ meV. The deepest minima in the density of states occur at fields where E_F moves abruptly from a Landau level associated with one subband to a Landau level associated with the other subband, as between peaks P and Q in Fig. 3(b). The characteristic feature, however, which is observed experimentally, is the triplet of peaks Q,R,S or T,U,V. The middle peak R occurs when the $E_{1,0^-}$ and $E_{0,2^-}$ Landau levels coincide, as approximately happens in Fig. 2(e). From Eq. (1), at that value of B

$$E_1-E_0=N\hbar\omega_c(B)\ . \quad (6)$$

Since N is known, E_1-E_0 can be determined. In the

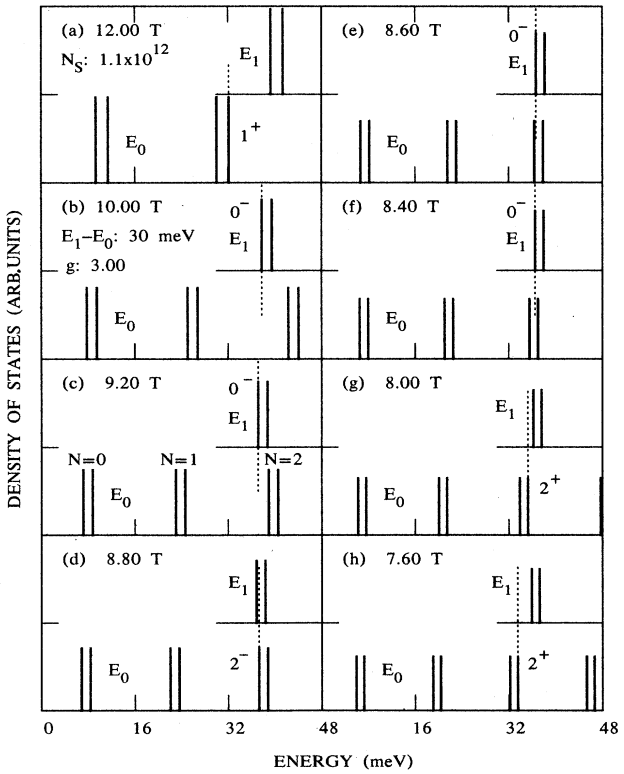

FIG. 2. Schematic energy dependence of density of states of two subbands of a 2D EG in an accumulation layer in different perpendicular magnetic fields. Dotted lines show E_F at each B. Vertical lines are proportional to degeneracy of each spin-split Landau level.

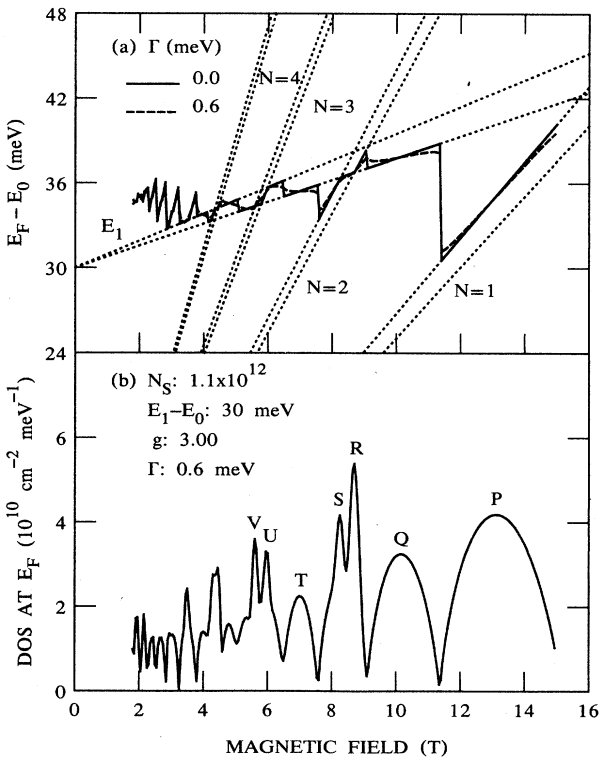

FIG. 3. (a) Dependence of Fermi energy on magnetic field for ideal Landau level diagram of Fig. 2. Dotted lines show spin-split Landau levels of different subbands. Dashed line includes effect of Gaussian broadening of Landau levels on E_F. (b) Dependence of density of states at E_F on magnetic field for Gaussian broadening of Landau levels.

same way the triplet of peaks T, U, and V occurs when the $N=3$ Landau level moves in energy below the 0^- Landau level of the first excited subband, and a third triplet can be resolved when the $N=4$ Landau level passes through the $E_{1,0^-}$ Landau level.

The values of N_S and E_1-E_0 in Fig. 2 and 3 are appropriate for the AlGaAs capacitor studied in the present work. The value of g and Γ are arbitrary but are reasonable. The proper value of g to use is uncertain. Values of g for GaAs heterostructures reported in the literature range from 0.19 to 19.[35–40] For bulk GaAs, g is -0.44.[41] In 2D EG layers there is evidence for exchange enhancement of the g value. Englert *et al.*[36] reported that g oscillates between 0.52 when E_F lies between two Landau levels and a maximum of ~ 5 when E_F lies between two completely separate spin levels. Smith *et al.*[28] used a value of g that depended on B in deriving the density of states from magnetocapacitance measurements. In both cases modulation-doped structures were used. There are no reported values of g for an accumulation layer though magnetotunneling and magnetocapacitance measurements show that g is enhanced over its bulk value.[22] The arguments of Fig. 2 and Fig. 3 for deriving E_1-E_0 are not sensitive to the value of g that is chosen, for $g\sim 3-9$. It is assumed, however, that g is the same for both subbands. The dashed line in Fig. 3(a) shows the Fermi energy for the DOS diagram in Fig. 3(b). The Fermi energy deviates from that calculated for δ-function Landau levels in some ranges of B but it coincides with the ideal E_F when the Landau levels from upper and lower subbands coincide.

The value of Γ used in Fig. 3, 0.6 meV, is chosen because the peaks in the DOS in Fig. 3 remain well resolved. If Γ is made larger, peaks are still observed but are not as well resolved. Ando and Murayama[42] have calculated the broadening of Landau levels and its dependence on the position of E_F relative to the Landau level. Theoretically Γ is larger when the Fermi level is between Landau levels than when it is in the middle of a Landau level. Their calculated values of Γ are in the range of 0.6 meV as used in Fig. 3. Larger values of Γ and values of Γ that depend on $\sqrt{B}$ have been used to fit specific heat, magnetization, and magnetocapacitance measurements of the DOS in modulation-doped heterostructures.[23]

EXPERIMENTAL

Figure 1(a) shows schematically the structure and energy level diagram of the AlGaAs capacitor studied. The sample was grown by molecular beam epitaxy on a ⟨100⟩-oriented, n^+-type GaAs wafer. The n^--type GaAs layer is ~ 1 μm thick. The properties of the sample measured, sample A of Ref. 43, and the procedures used to measure capacitance-voltage (C-V) and the conductance-voltage (G-V) curves have been described elsewhere.[22,43] An ac modulation voltage of 0.004 V rms is used for measurements. The sample area is 4.13×10^{-4} cm^2. Magnetic field measurements up to 15 T were made in a superconducting magnet with the sample immersed in pumped liquid helium, and with the magnetic field perpendicular to the sample.

RESULTS

C-V curves for sample A at 1.6 K, 100 kHz, and different magnetic fields are shown in Fig. 4. For sample A at 0 T, $V_{FB}=-0.030$ V; an accumulation layer forms on n^--type GaAs for larger V_G. There is a characteristic decrease in capacitance as V_G increases above ~ 0.1 V due to band bending in the n^+ gate; the magnitude of the decrease can be used to estimate gate doping.[21]

In C-V curves such as in Fig. 4 one establishes a pattern of Landau levels whose spacing is determined by B. Increasing V_G increases N_S, increases E_F, and therefore moves E_F through successive Landau levels. At 2 T the sequence of maxima and minima shows many Landau levels. The observation that the maximum C is higher than at 0 T is consistent with the density of states at the peak of the Landau levels being greater than at 0 T. At 4 T, indications of spin splitting appear. The maximum capacitance decreases because magnetic localization of carriers in the n^--type GaAs substrate increases the series resistance and reduces the measured values of C.[22,43] At 6 T, spin splitting is pronounced. At higher values of B, magnetic localization of electrons in the n^--type GaAs substrate is nearly complete;[43] the measured C is almost completely suppressed by series resistance for $V_G \lesssim 0.3$ V. The minimum capacitance is approximately constant for $-1.0V < V_G \lesssim 0.25$ V and is that of ~ 1 μm of GaAs plus 23 nm of $Al_xGa_{1-x}As$. For $V_G \gtrsim 0.3$ V, C increases rapidly; its value is not reduced by series resistance of the n^--type GaAs substrate for $V_G \gtrsim 0.4$ V. This occurs be-

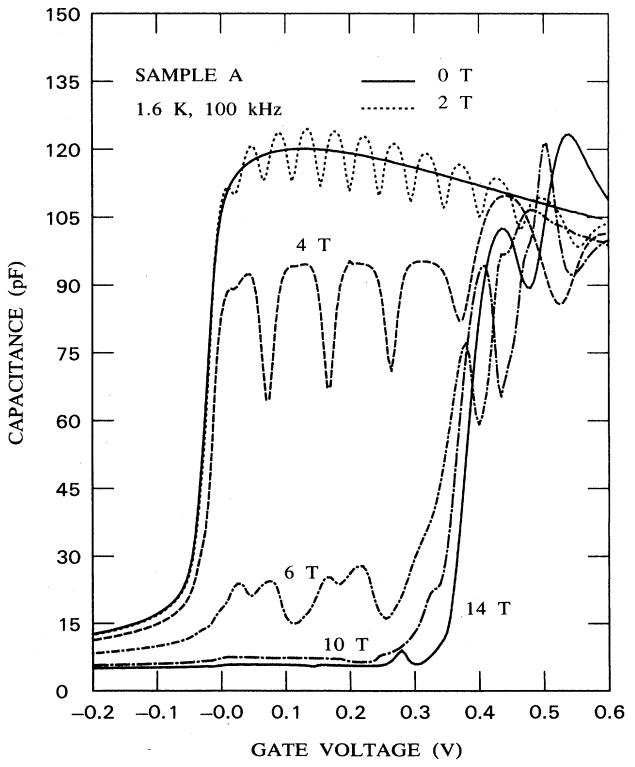

FIG. 4. Capacitance-voltage curves of sample A at 100 kHz and different perpendicular magnetic fields.

cause dc tunnel currents become the dominant component of ac conductance and lower the effective ac series resistance of the n^--type GaAs substrate.[43]

C-V-B curves in which V_G is maintained constant and *C* is measured while *B* is swept are shown for sample *A* in Figs. 5 and 6. The ratio of capacitance at *B* to capacitance at $B=0$ T is plotted versus *B* for different values of V_G. The curves are complementary to the *C-V* curves of Fig. 4. The constant V_G establishes a nearly constant N_S in the accumulation layer; changing *B* moves a succession of Landau levels through the Fermi level. The experimental situation corresponds closely to that of Figs. 2 and 3. At low *B*, $B \lesssim 5.5$ T, *C-V-B* curves of sample *A* at any V_G are characterized by a series of capacitance minima which are equivalent to Shubnikov–de Haas (SdH) minima in conductance curves of heterostructures. The position of minima is proportional to $1/B$. By assuming that each capacitance minimum corresponds to the passage of a complete Landau level through E_F, Eq. (2) can be used to determine the surface concentration at V_G. Figure 7 shown N_S derived from Fourier analysis of *C-V-B* curves such as those of Figs. 5 or 6. Evaluation of N_S from Eq. 2 assumes that only one subband is occupied. This is the case at least for $V_G \lesssim 0.32$ V for sample *A*.

The *C-V-B* curves of Fig. 5 are measured at 10 kHz to minimize the reduction of capacitance by series resistance due to magnetic localization of electrons in n^--type GaAs. Series resistance becomes important for $B \gtrsim 6$ T as shown by the decrease in capacitance ratio at higher *B*. *C-V-B* curves for Fig. 5 were only measured to 9.5 T because of distortion of the curves by series resistance.

C-V-B curves at 100 kHz for $0.32\ \text{V} \leq V_G \leq 0.52$ V are shown in Fig. 6. At 0.32 V series resistance reduces *C* for $B \gtrsim 4$ T; a spin-split minimum is seen at ~ 9 T, in addition to a sequence of Landau level minima at lower *B*. At $V_G \gtrsim 0.36$ V the effect of magnetic localization of electrons in the n^--type GaAs substrate becomes small, as shown in the *C-V* curves of Fig. 4 by the rise of the minimum capacitance for $B > 6$ T and increasing V_G. For $V_G \gtrsim 0.44$ V there is essentially no reduction of capacitance ratio by series resistance.

The striking feature of *C-V-B* curves for sample *A* is

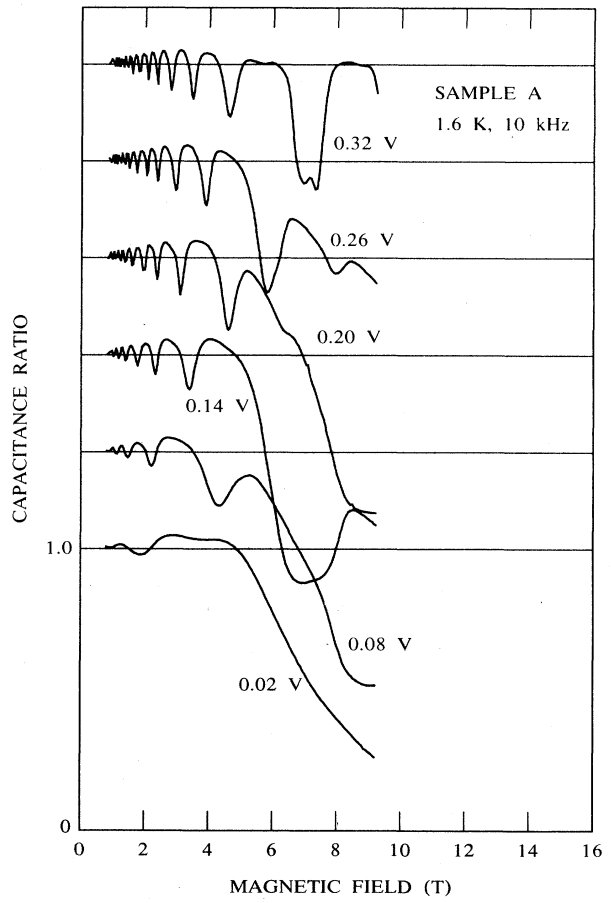

FIG. 5. Dependence of the ratio of capacitance at magnetic field *B* to the capacitance at 0 T on *B*, for different values of V_G for sample *A*. Curves are shifted for clarity. Horizontal lines show capacitance ratio = 1.0. 10 kHz.

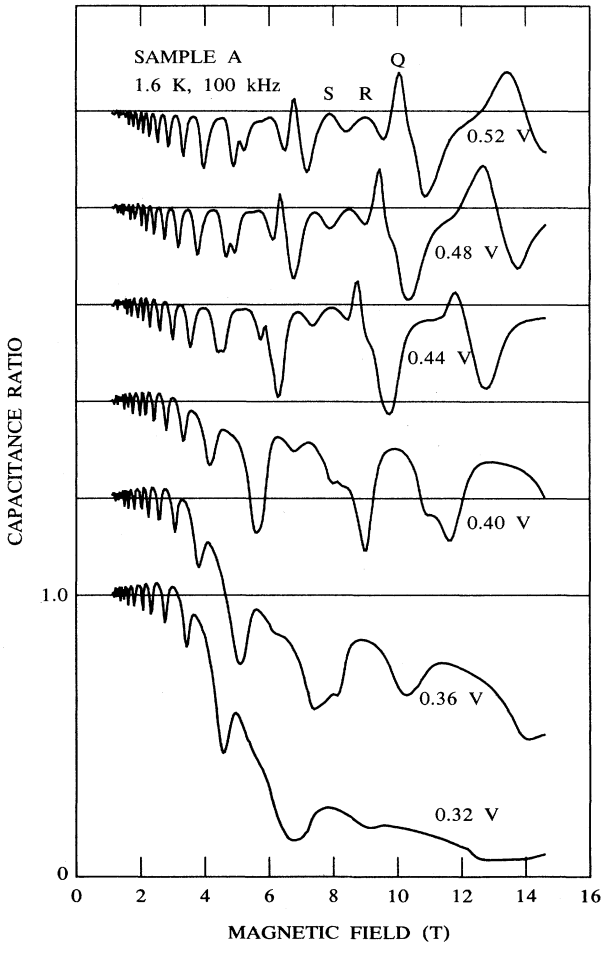

FIG. 6. Dependence of the ratio of capacitance at magnetic field *B* to the capacitance at 0 T on *B* for different values of V_G for sample *A*. Curves are shifted for clarity. Horizontal lines show capacitance ratio = 1.0. 100 kHz.

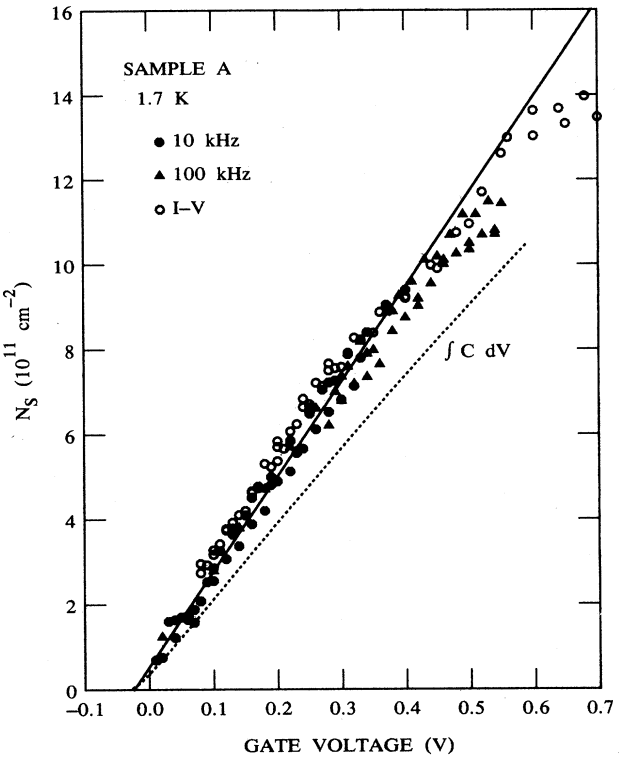

FIG. 7. Dependence of electron concentration in accumulation layer of Sample A on V_G from Fourier analysis of C-V-B or I-V-B curves. Solid line is least-squares fit of C-V-B data for $0.02 \leq V_G \leq 0.32$ V.

the triplet structure, three maxima designed as Q, R, and S in the curve for $V_G = 0.52$ V. The structure is repeated twice at lower B. The similarity to Fig. 3(b) leads us to associate the middle maximum R with the magnetic field at which the energy of the 2^- level of the lower subband coincides with the 0^- level of the first excited subband. Correspondingly the triplet structure at 6 T and at 4.5 T correspond to the $N=3$ and $N=4$ Landau levels coinciding with the $E_{1,0^-}$ level. At lower values of V_G the triplet structure shifts to lower B but is still observable at $V_G = 0.36$ V. Fourier analysis of C-V-B curves at 100 kHz and $B \lesssim 5$ T have also been used to derive N_S; the points are labeled in Fig. 7.

Earlier work has shown that I-V-B curves in which the ratio of dc tunnel currents at B to tunnel currents at 0 T for a constant V_G are plotted as a function of B can be analyzed to give N_S.[22] The open circles in Fig. 7 are derived from Fourier analysis of such I-V-B curves. The solid line is the least-squares fit of C-V-B data for $0.02 \text{ V} \leq V_G \leq 0.32$ V. V_{FB} from the intercept of Fig. 7, -0.024 V, agrees well with V_{FB} derived from I-V curves or C-V curves such as those of Fig. 4.[43] N_S derived from C-V-B or I-V-B curves on the assumption that only one subband is occupied, deviates from the solid line for $V_G \gtrsim 0.35$ V. This is consistent with the observation of a triplet structure in C-V-B curves at V_G as low as 0.36 V which is associated with occupation of the first excited subband. The voltage period of capacitance minima in the C-V curve at 2 T in Fig. 4 also increases when $V_G \gtrsim 0.35$ V, indicating that carriers occupy a second subband. The value of N_S at 0.32 V, $\sim 7\times10^{11}$ cm^{-2}, is larger than the value predicted for occupation of the first excited subband of an accumulation layer to occur, $\sim 3\times10^{11}$ cm^{-2}.[10,11] However, the theoretical values depend on the value of depletion charge in n^--type GaAs which is not known for sample A. The data of Fig. 7 are not accurate enough to detect higher subband occupancy at lower N_S. The dotted lines shows $N_S = \int C\, dV$ for the C-V curve at 0 T in Fig. 4. As has been reported before,[22] N_S from SdH oscillations in C-V-B or I-V-B curves consistently gives higher values of N_S than integration of C-V curves. The discrepancy is more pronounced for $N_G < 1\times10^{18}$ cm^3 than for higher gate doping, but the reason for the discrepancy is not known.

Figure 8(a) shows the subband separation, $E_1 - E_0$, derived from C-V-B curves. The Landau level of the lowest subband whose coincidence with the 0^- Landau level of the first excited subband is used to determine $E_1 - E_0$ is identified. The abscissa is V_G; values of N_S corresponding to each value of V_G are obtained from the least-squares fit of C-V-B data in Fig. 7. The dashed line is from Ando, the dotted curve is from Stern and Das Sar-

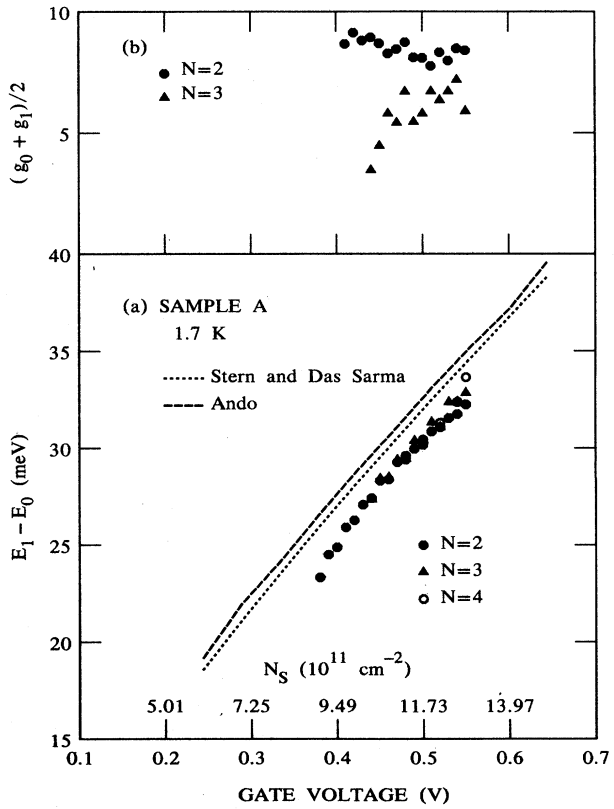

FIG. 8. (a) Subband energy separation, $E_1 - E_0$, for sample A in accumulation as a function of V_G, and of N_S. Dashed line from Ref. 10, $N_{depl} = 1\times10^9$ cm^{-2}; dotted line from Ref. 11, $N_{depl} = 3.2\times10^9$ cm^{-2}. (b) $(g_0+g_1)/2$ as a function of V_G, calculated from magnetocapacitance curves at 100 kHz.

ma.[10,11] The depletion charge used for the calculation differs for the two curves; the value is given in the figure caption. Both curves parallel experimental data but are shifted from experiment. The slope of experimental and theoretical curves is nearly identical. The discrepancy may be due to differences in depletion charge of sample *A* from that assumed in the calculations; it may also be due to experimental uncertainties in N_S and E_1-E_0.

Structure due to Landau levels is observed in *I-V-B* curves at $B \lesssim 6$ T; structure due to coincidence of Landau levels in the E_1 and E_0 levels is also seen in *I-V-B* curves, as shown in Fig. 9. In Fig. 9, *C-V-B*, *I-V-B*, and *dI/dB-V-B* curves are shown for $V_G=0.48$ V and 0.44 V. For *I-V-B* curves the ratio plotted is the ratio of current at *B* to the current at 0 T for a given V_G. For *C-V-B* curves the ratio is the ratio of capacitance at *B* to capacitance at 0 T for V_G. In each case the top curve shows the capacitance ratio, the middle curve shows the current ratio, and the bottom curve shows the derivative of the current ratio with respect to *B*. The derivative has peaks at values of *B* that are close to maxima in the capacitance ratio. Structure in *I-V-B* curves due to overlap of Landau levels in two subbands is less pronounced than in *C-V-B* curves but it is detectable. In some cases it may be possible to measure E_{10} from *I-V-B* curves at higher values of V_G than can be used for *C-V-B* curves.

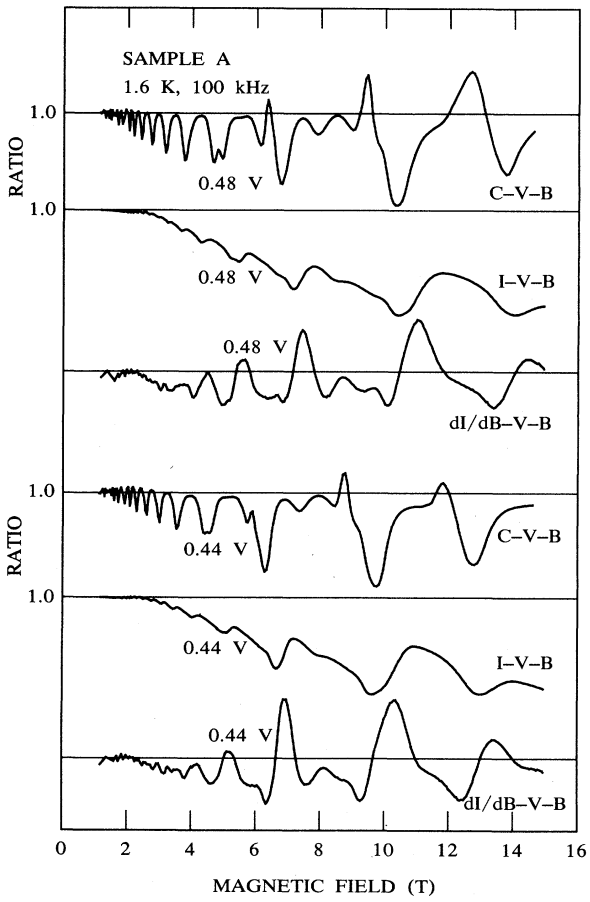

FIG. 9. *C-V-B* curves at 100 kHz, and dc *I-V-B* and *dI/dB-V-B* curves for two values of V_G for sample *A*.

DISCUSSION

The use of magnetocapacitance measurements provides a new method of determining E_1-E_0 as a function of N_S for an accumulation layer on n^--type GaAs. *C-V-B* measurements by themselves only determine the magnetic fields at which maxima or minima in the density of states occur; they do not inherently provide an energy scale in the way that optical measurements do. According to the model of Figs. 2 and 3, the conversion of magnetic field to an energy scale relies on three assumptions. One assumption is that E_1-E_0 at a given N_S is independent of magnetic field; the second is that m^* is known and is the same for both subbands; and the third is that g is the same in both subbands when the 0^- level of the upper subband and the N^- level of the lower subband coincide.

The assumption that E_1-E_0 is constant in a perpendicular magnetic field is a good one. It is well known that there is a diamagnetic shift of E_1 with respect to E_0 when *B* is parallel to an accumulation or inversion layer.[1,44,45] Such a shift can lead to magnetic depopulation of subbands in parallel magnetic fields. The subband shift is small, even in large magnetic fields, and is not significant for magnetic fields perpendicular to an accumulation layer. The constancy of m^* is also a reasonable assumption, and with it the constancy of $\hbar\omega_c$, the Landau level separation. There is some evidence that non-parabolicity of the conduction band affects m^* when E_F is large, and also for fluctuations in m^* when occupation of Landau levels is complete.[19] However, such effects are less than 5% of the value of m^*; the correction to the data of Fig. 8(a) would be small.

The equality of g for the two subbands when they overlap is more problematic. The large values of g observed experimentally in modulation-doped heterostructures are due to exchange interactions among electrons that enhance the g value in a 2D EG over that observed in bulk. Ando and Uemura[46] showed that g should oscillate in strong magnetic fields. Englert *et al.*[36] and Smith *et al.*[28] used an expression for g of the form

$$g=g_e+\frac{E_{\rm ex}}{\mu_B B}\sum_N (n_{N\uparrow}-n_{N\downarrow}) , \tag{7}$$

where g_e is the free-electron g value for GaAs, $E_{\rm ex}$ is the exchange parameter, and $n_{N\uparrow\downarrow}$ are the occupation factors of the spin levels. g is the maximum when E_F lies between spin-split Landau levels. In deriving E_{10} from Eq. (6), the 0^- level of the first excited subband coincides with the N^- level of the lowest subband. At coincidence the term $(n_{N\uparrow}-n_{N\downarrow})$ in Eq. (7) should be nearly equal for each spin-split level. Equality of the g value of each subband then depends on $E_{\rm ex}$ being equal for the two subbands. No calculations of $E_{\rm ex}$ are available for accumulation layers on GaAs, but the approximation that g is equal for the two subbands is reasonable, particularly

since $g\mu_B B$ is small compared to $\hbar\omega_c$.

For the simple model of Figs. 2 and 3, peak S of Fig. 3(b) is where the $E_{1,0^-}$ and $E_{0,2^+}$ levels coincide. From Eq. (1), if g_0 and g_1 are g values for electrons in the E_0 and E_1 subbands, respectively,

$$\frac{g_0+g_1}{2}=\frac{[E_1-E_0-N\hbar\omega_c(B_S)]}{\mu_B B_S}, \tag{8}$$

where B_S is the value of B corresponding to peak S. In principal, $(g_0+g_1)/2$ can be obtained from Eq. (8) since E_1-E_0 is determined from peak R of Fig. 6. Values of $(g_0+g_1)/2$ are plotted in Fig. 8(b) for the two Landau levels of E_0, $N=2^+$ and $N=3^+$, for which structure can be resolved. For $N=2$, the average value of $(g_0+g_1)/2$ is 8,5 and is fairly constant. For $N=3$ there is a greater scatter of the data but the values of $(g_0+g_1)/2$ are mostly in the range of 6 to 7; they are consistently lower than for the $N=2$ Landau level. Since B_S is lower when $N=3$, the difference in occupation of subbands in Eq. (7) is greater when $N=2$ than when $N=3$. These values of g are significantly larger than the values of 2.0 to 4.0 used by Englert *et al.*[36] and Smith *et al.*[28] in analyzing SdH data on modulation-doped heterostructures. However, the values of N_S and of B are also higher and little is known about the nature of spin splitting in a 2D EG when two subbands are occupied.

It is difficult to compare E_1-E_0 in Fig. 8(a) with previous results.[9,13–20] The values of N_S at which E_1-E_0 is determined are higher and cover a wider range of N_S than has generally been possible with modulation-doped heterostructures. Abstreiter[13] found $E_{10}\sim 22$ meV for $N_S=1\times10^{12}$ cm^{-2} which is lower than the value, ~ 27 meV, found here. Some samples measured by Wieck *et al.*[17] would agree with Fig. 8(a) but the dependence of E_{10} on N_S is less steep than in Fig. 8(a). Other measurements of E_{10} are at lower values of N_S.

Comparison of an experimental C-V-B curve with ideal C-V-B curves calculated from Eqs. (1)–(5) shows some agreement with theory as well as some uncertainties. From the least-squares fit of C-V-B data for $V_G\leq 0.32$ V, $N_S=1.2\times10^{12}$ cm^{-2} for $V_G=0.51$ V. Figure 10(a) shows the C-V-B curve for $V_G=0.51$ V. Figure 10(d) shows a calculated C-V-B curve for $N_S=1.2\times10^{12}$ cm^{-2}, $E_1-E_0=31$ meV, $\Gamma=1.0$ meV, and $g=4.0$. Values of C_I and C_G in Eq. (3) were obtained by modeling C-V curves at 0 T.[24,47] The measured capacitance at 0 T was then used to determine $1/C_S$; the value of $\gamma z_0/\epsilon_S$ in Eq. (4) was obtained from $1/C_S$ by assuming that the density of states was that at 0 T.[29] The plotted capacitance ratio is the ratio of the calculated capacitance at B to the experimental value at 0 T.

For $N_S=1.2\times10^{12}$ cm^{-2}, structure in C-V-B curves does not correspond closely to experiment. Additional structure arises because the Fermi level stays mainly in the $E_{1,0^-}$ or $E_{1,0^+}$ levels for $B\lesssim 12$ T rather than shifting between the 0^- level of the first excited subband and Landau levels of the lowest subband. In addition, the minimum at L, the value of B where the Fermi level shifts from the $E_{0,1^+}$ level to the $E_{1,0^-}$ level, is about 1 T higher than in the experiment.

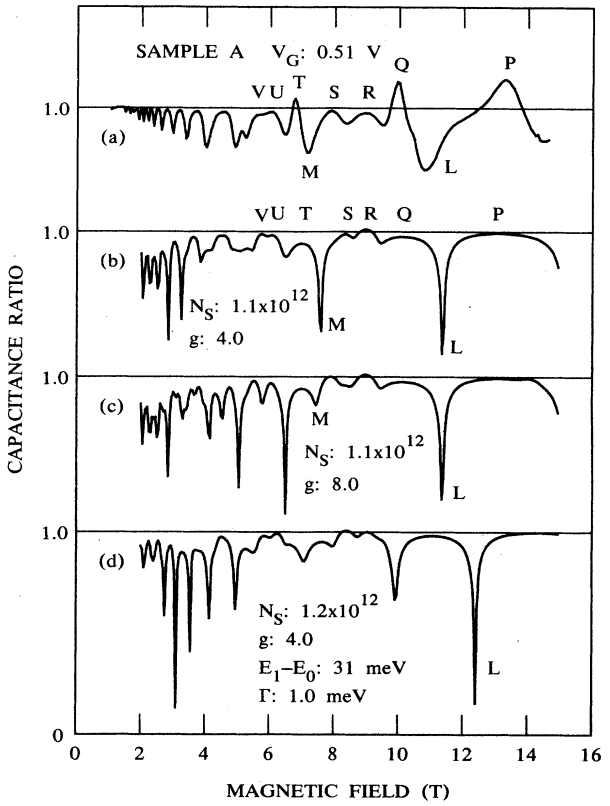

FIG. 10. Comparison of experimental and calculated C-V-B curves. (a) Experimental C-V-B curve for $V_G=0.51$ V. (b), (c), and (d) Calculated C-V-B curves for parameters given on the figure. E_1-E_0 and Γ are constant for the three curves.

A closer fit between experimental and theoretical C-V-B curves is found for $N_S=1.1\times10^{12}$ cm^{-2}. Figures 10(b) and 10(c) show calculated C-V-B curves for $N_S=1.1\times10^{12}$ cm^{-2}, the same E_1-E_0 and Γ as Fig. 10(d), and two different values of g. The separation of Landau minima, $L-M$, is close to the experimental value though the values of B for both minima are slightly higher than experiment. The spacing of the triplet Q, R, S for $g=8.0$ is close to experiment, consistent with values of $(g_1+g_0)/2$ of ~ 8.5 in Fig. 8(b). In Fig. 10(b) the triplet T, U, V for $g=4.0$ and also structure at lower B is close to that of experiment.

The discrepancy in N_S between the value at $V_G=0.51$ V from Fig. 7, 1.2×10^{12} cm^{-2}, and the value of N_S, 1.1×10^{12} cm^{-2}, that gives closer agreement between calculated and experimental C-V-B curves is within the spread of experimental data. It suggests that the least-squares fit of C-V-B data for $V_G<0.32$ V gives values of N_S that are too high for V_G between 0.4 and 0.55 V. If this is the case the agreement between experiment and theory in Fig. 8(a) becomes even closer. Although the calculated C-V-B curves reproduce structure in experimental curves well, there are clearly some differences. Experimentally, peaks Q and T are more pronounced than peak R or U which is where the sum of peaks from Landau levels in two subbands should be the largest. Ex-

perimental minima are less sharp than calculated minima; this is a function of the broadening Γ which is taken to be independent of B for calculations. If Γ is larger, the calculated minima are less pronounced. Structure between L and P of experimental curves is not present in calculated curves; its origin is uncertain, but it may be due to the Fermi level being pinned in localized states of the $E_{0,1^-}$ Landau level rather than moving smoothly through the Landau level as B changes. Considering the assumptions involved in calculating ideal C-V-B curves, the agreement between theory and experiment is reasonable.

There are limitations on the use of magnetocapacitance curves to determine subband separations. If dc tunnel currents are large, ac conductance of an AlGaAs capacitor becomes large and it is not possible to measure capacitance accurately. At a given value of $V_G - V_{FB}$, N_S is proportional to $1/d$ where d is the insulator thickness. dc tunnel currents are exponentially proportional to $1/d$. If the undoped $Al_xGa_{1-x}As$ layer is too thin or the barrier height at the $GaAs/Al_xGa_{1-x}As$ interface is too small due to low values of x, tunnel currents can become large before the first excited subband is occupied, and $E_1 - E_0$ cannot be determined. If $E_1 - E_0$ is too small at a given value of N_S, the 0^+ level of the first excited subband can be occupied. Shifting of the Fermi level between $E_{1,0^-}$ or $E_{1,0^+}$ levels and spin-split Landau levels of the lowest subband can produce a pattern of maxima in magnetocapacitance curves that is difficult to interpret in terms of overlap of Landau levels in the two subbands. In such a case the relatively simple triplet structure of Fig. 6 may not be observed.

However, if conditions are favorable, as in sample A, magnetocapacitance curves are the simplest method of determining subband separation as a function of surface carrier concentration N_S. N_S can easily be varied over a wider range than is possible with modulation-doped heterostructures; it can also be determined from C-V curves, as can other sample properties such as barrier heights, dielectric thickness, substrate doping, and gate doping that are needed to characterize the system.

ACKNOWLEDGMENTS

It is a pleasure to acknowledge discussions with F. Stern, T. P. Smith III, and F. F. Fang. F. Stern calculated the theoretical curve of Fig. 8, and carefully read the manuscript. The Fourier-analysis program was kindly provided by J. W. Stasiak. H. Morkoç of the University of Illinois at Urbana-Champaign provided the sample. The work would not have been possible without the use of F. F. Fang's superconducting magnet.

[1]For a review see T. Ando, A. B. Fowler, and F. Stern, Rev. Mod. Phys. **54**, 437 (1982).
[2]H. L. Störmer, A. C. Gossard, and W. Wiegmann, Solid State Commun. **41**, 707 (1982).
[3]Th. Englert, J. C. Maan, D. C. Tsui, and A. C. Gossard, Solid State Commun. **45**, 989 (1983).
[4]K. Tsubaki, A. Livingstone, M. Kawashima, H. Okamoto, and K. Kumabe, Solid State Commun. **46**, 517 (1983).
[5]J. J. Harris, D. E. Lacklison, C. T. Foxon, F. M. Selten, A. M. Suckling, R. J. Nicholas, and K. W. J. Barnham, Semicond. Sci. Technol. **2**, 783 (1987).
[6]H. van Houten, J. G. Williamson, M. E. I. Broekaart, C. T. Foxon, and J. J. Harris, Phys. Rev. B **37**, 2756 (1988).
[7]T. P. Smith III and F. F. Fang, Phys. Rev. B **37**, 4303 (1988).
[8]F. F. Fang, T. P. Smith III, and S. L. Wright, Surf. Sci. **196**, 310 (1988).
[9]T. P. Smith, III, F. F. Fang. U. Meirav, and M. Heiblum, Phys. Rev. B **38**, 12 744 (1988).
[10]T. Ando, J. Phys. Soc. Jpn. **51**, 3893 (1982).
[11]F. Stern and S. Das Sarma, Phys. Rev. B **30**, 840 (1984), and private communication.
[12]M. Tomak and V. E. Godwin, Phys. Status Solidi B **137**, 183 (1986).
[13]G. Abstreiter, Surf. Sci. **98**, 117 (1980).
[14]A. Pinczuk, J. M. Worlock, H. L. Störmer, R. Dingle, W. Wiegmann, and A. C. Gossard, Solid State Commun. **36**, 43 (1980).
[15]Z. Schlesinger, J. C. M. Hwang, and S. J. Allen, Phys. Rev. Lett. **50**, 2098 (1983).
[16]G. L. J. A. Rikken, H. Sigg, C. J. G. M. Langerak, H. W. Myron, J. A. A. J. Perenboom, and G. Weimann, Phys. Rev. B **34**, 5590 (1986).
[17]A. D. Wieck, J. C. Mann, U. Merkt, J. P. Kotthaus, K. Ploog, and G. Weimann, Phys. Rev. B **35**, 4145 (1987).
[18]K. Ensslin, D. Heitmann, H. Sigg, and K. Ploog, Phys. Rev. B **36**, 8177 (1987).
[19]K. Ensslin, D. Heitmann, H. Sigg, and K. Ploog, Surf. Sci. **196**, 263 (1988).
[20]K. Ensslin, D. Heitmann, and K. Ploog, Phys. Rev. B **37**, 10150 (1988).
[21]T. W. Hickmott, P. M. Solomon, R. Fischer, and H. Morkoç, J. Appl. Phys. **57**, 2844 (1985).
[22]T. W. Hickmott, Phys. Rev. B **32**, 6531 (1985).
[23]For reviews, see J. P. Eisenstein, Phys. Scr. **114**, 42 (1986); E. Gornik, in *The Physics of the Two-Dimensional Electron Gas,* edited by J. T. Devreese and F. M. Peeters (Plenum, New York, 1987), p. 365.
[24]T. W. Hickmott, P. M. Solomon, R. Fischer, and H. Morkoç, Appl. Phys. Lett. **44**, 90 (1983).
[25]A. M. Voshchenkov and J. N. Zemel, Phys. Rev. B **9**, 4410 (1974).
[26]F. Stern, IBM Internal Report No. RC-3758, 1972 (unpublished).
[27]T. P. Smith III, B. B. Goldberg, P. J. Stiles, and M. Heiblum, Phys. Rev. B **32**, 2696 (1985).
[28]T. P. Smith III, W. I. Wang, and P. J. Stiles, Phys, Rev. B **34**, 2995 (1986).
[29]V. Mosser, D. Weiss, K. v. Klitzing, K. Ploog, and G. Weimann, Solid State Commun. **58**, 5 (1986).
[30]D. Weiss and K. v. Klitzing, in *High Magnetic Fields in Semiconductor Physics,* Vol. 71 of *Springer Series in Solid State Science,* edited by G. Landwehr (Springer, Berlin, 1987), p. 57.
[31]D. Shoenberg, J. Low Temp. Phys. **56**, 417 (1984).
[32]J. C. Portal, R. J. Nicholas, M. A. Brummell, A. Y. Cho, K.

Y. Cheng, and T. P. Pearsall, Solid State Commun. **43**, 907 (1982).
[33]V. I. Nizhankovskii, V. G. Mokerov, B. K. Medvedev, and Yu. V. Shaldin, Zh. Eksp. Teor. Fiz. **90**, 1326 (1986) [Sov. Phys.—JETP **63**, 776 (1986).]
[34]A. M. Dabiran, R. T. Zeller, F. F. Fang, S. L. Wright, and P. J. Stiles, Surf. Sci. **196**, 712 (1988).
[35]S. Narita, S. Takeyama, W. B. Luo, S. Hiyamizu, K. Nanbu, and H. Hashimoto, Jpn. J. Appl. Phys. **20**, L861 (1981).
[36]Th. Englert, D. C. Tsui, A. C. Gossard, and Ch. Uihlein, Surf. Sci. **113**, 295 (1982).
[37]R. J. Nicholas, M. A. Brummell, and J. C. Portal, Surf. Sci. **113**, 290 (1982).
[38]D. Stein, K. v. Klitzing, and G. Weimann, Phys. Rev. Lett. **51**, 130 (1983).
[39]A. Raymond, J. L. Robert, C. Bousquet, W. Zawadzki, F. Alexandre, and I. M. Masson, Solid State Commun. **55**, 271 (1985).
[40]M. Dobers, K. v. Klitzing, and G. Weimann, Phys. Rev. B **38**, 5453 (1988).
[41]C. Weisbuch and C. Hermann, Phys. Rev. B **15**, 816 (1977).
[42]T. Ando and Y. Murayama, J. Phys. Soc. Jpn. **54**, 1519 (1985).
[43]T. W. Hickmott, Phys. Rev. B **38**, 12 404 (1988).
[44]K. F. Berggren and D. J. Newson, Semicond. Sci. Technol. **1**, 327 (1986).
[45]M. A. Brummell, M. A. Hopkins, R. J. Nicholas, J. C. Portal, K. Y. Cheng, and A. Y. Cho, J. Phys. C **19**, L107 (1986).
[46]T. Ando and Y. Uemura, J. Phys. Soc. Jpn. **37**, 1044 (1974).
[47]The program used for *C-V* calculations at low temperatures was provided by F. Stern. It is a continuum model which includes no quantum effects.